




Characterisation of internal oxygen concentration of strawberry (*Fragaria × ananassa*) and blueberry (*Vaccinium corymbosum*)

Zeyu Xiao^{A,B,C,*} , Stephen D. Tyerman^{A,B,D} , Timothy Stait-Gardner^C , William S. Price^C ,
Vinay Pagay^{A,D} , Leigh M. Schmidtke^{A,B}  and Suzy Y. Rogiers^{A,B,C,E} 

For full list of author affiliations and declarations see end of paper

***Correspondence to:**

Zeyu Xiao
Gulbali Institute, Charles Sturt University,
Wagga Wagga, NSW 2678, Australia
Email: zxiao@csu.edu.au

Handling Editor:

Sergey Shabala

Received: 26 August 2021

Accepted: 20 November 2022

Published: 16 December 2022

Cite this:

Xiao Z *et al.* (2023)
Functional Plant Biology, **50**(3), 256–265.
doi:[10.1071/FP21259](https://doi.org/10.1071/FP21259)

© 2023 The Author(s) (or their employer(s)). Published by CSIRO Publishing.

This is an open access article distributed under the Creative Commons Attribution-NonCommercial-NoDerivatives 4.0 International License ([CC BY-NC-ND](https://creativecommons.org/licenses/by-nc-nd/4.0/)).

OPEN ACCESS

ABSTRACT

Gas exchange mechanisms play crucial roles in maintaining fruit post-harvest quality in perishable fruit such as strawberry (*Fragaria × ananassa* Duch.) and blueberry (*Vaccinium corymbosum* L.). The internal oxygen concentration ([O₂]) of strawberry and blueberry were measured using Clark-type oxygen sensing electrodes. The volume of intercellular voids in strawberry was obtained by micro-computed tomography (micro-CT). In both berries, internal [O₂] was consistent and relatively high across measured tissues. The overall [O₂] was well above the Michaelis constant (K_m) for cytochrome c oxidase in both fruit and different from previously examined grape (*Vitis vinifera* L.) berry mesocarp with near zero minimum [O₂]. In strawberry and blueberry, cell vitality was also maintained at full maturity in the mesocarp. Higher storage temperature (i.e. 20 vs 4°C) reduced internal [O₂] of strawberry. Pedicel detachment in blueberry was associated with greater fruit dehydration and lower internal [O₂] after short-term storage of 12 h. The results suggest that the intercellular voids of the fruit's mesocarp provide an efficient gas exchange route for maintaining high fruit internal [O₂] post-harvest.

Keywords: 3D microstructure, *Fragaria × ananassa*, intercellular voids, micro-CT, modified storage conditions, oxygen measurement, post-harvest, *Vaccinium corymbosum*.

Introduction

Strawberry (*Fragaria × ananassa* Duch.) and blueberry (*Vaccinium corymbosum* L.) fruit are harvested when fully ripe, and both are susceptible to perishing rapidly post-harvest. Both benefit from modified storage conditions post-harvest that improves storability (Kader and Ben-Yehoshua 2000). This commonly involves managing the concentration of atmospheric oxygen ([O₂]) and carbon dioxide ([CO₂]), as well as the storage temperature (Schotsmans *et al.* 2007; Aday *et al.* 2011; Chiabrando and Giacalone 2011; Rodriguez and Zoffoli 2016). Elevated [CO₂] can greatly reduce fungal attack (Brown 1922); however, fruit internal [O₂] must be maintained to prevent anaerobic fermentation and off-flavour generation (Ke *et al.* 1991; Beaudry *et al.* 1992; Larsen and Watkins 1995; Pott *et al.* 2020).

Fruit relies on the intercellular air spaces to provide the main route for diffusive transport of gases. Due to low solubility in water, O₂ transport occurs mainly through air spaces in the fruit parenchyma (i.e. intercellular voids) and less in the intracellular liquid (Ho *et al.* 2009). A study investigating the association between grape (*Vitis vinifera* L.) berry ripening and berry internal [O₂] found that the grape berry can develop a hypoxic (i.e. near zero [O₂]) mesocarp, as a consequence of the increased internal respiratory demand and restricted O₂ transport (Xiao *et al.* 2018a). Hypoxia in grape berries was associated with the decrease in mesocarp cell vitality in the berry during late ripening (Xiao *et al.* 2018a). Using micro computed tomography (micro-CT), a network of intercellular voids was also found connecting the pedicel and the locules (Xiao *et al.* 2018a). Furthermore, the porosity of the berry as a whole was found to decrease during late ripening, and this

was associated with a decrease in internal $[O_2]$ of the grape berry (Xiao *et al.* 2018b). The reduction in volume of intercellular voids could lead to a decrease in fruit internal $[O_2]$, which can affect fruit health.

Strawberry 'fruit' referred to in this study, in the botanical sense is the enlarged receptacle (Hollender *et al.* 2012). The fruit is harvested so that the pedicel remains attached to the fruit. In contrast, when harvesting the blueberry, fruit detachment can occur either at the pedicel–berry junction leaving a stem scar on the fruit or at the pedicel–peduncle junction so that the pedicel is retained (Vashisth and Malladi 2013). Significant post-harvest weight loss (i.e. 39–67%) occurs through the stem scar and sealing the scar experimentally with gas impermeable resin (i.e. nail polish) can reduce water loss and retain firmness (Moggia *et al.* 2017). Harvesting the blueberry with the pedicel attached as a strategy to minimise post-harvest weight loss should be further evaluated, and the question of how the removal of the pedicel affects fruit internal $[O_2]$ has not been addressed. A better understanding of the dynamics and factors regulating internal $[O_2]$ of the strawberry and blueberry fruit can assist horticultural improvement and post-harvest management.

In this study, the hypothesis that internal $[O_2]$ of the strawberries and blueberries at maturity remains relatively high, due to the presence of intercellular voids and/or locular cavities is tested. The internal $[O_2]$ changes during strawberry ripening were examined as well as how this responds to short-term storage in different temperatures. Internal $[O_2]$ and weight loss of blueberries at harvest and after short-term storage, with or without pedicel attached were also assessed. The intercellular voids (i.e. diffusion pathways of O_2 supply) within the cortex of strawberries were visualised and characterised by micro-CT.

Materials and methods

Plant materials

Fruit of cv. Albion strawberries (*Fragaria × ananassa* Duch.) were sampled from a commercial farm in Hahndorf, South Australia, in October 2018. Four randomised locations were allocated as replicates within the farm. The strawberries, sampled on the same day, were visually categorised into white, pink and red colour ripeness categories, transported immediately in an ice cooled box to the laboratory, stored at 4°C in the dark, and tested within 48 h of sampling at the Waite Campus, The University of Adelaide. Fruit internal $[O_2]$ were determined once the fruit temperature had re-equilibrated to ambient temperature (e.g. 20–22°C). Fresh weight and tissue vitality were determined. Total soluble solids (TSS) was measured using a digital refractometer (Atago, Tokyo, Japan). In December, a second batch of red strawberries were sampled from the same farm, transported immediately in an ice cooled box to the laboratory. These

red strawberries were stored, single layer, in unsealed plastic containers at either 20°C [84%, relative humidity (RH)] or 4°C (83%, RH) for 40 h. Fruit weight and internal $[O_2]$ were determined after storage once the fruit temperature had re-equilibrated to ambient temperature. Strawberries were also collected in December 2018 from another commercial farm in Thirlmere, New South Wales, for imaging by micro-CT at the Biomedical Magnetic Resonance Facility at the Western Sydney University node of the National Imaging Facility.

Fruit of cv. Nui blueberries (*Vaccinium corymbosum* L.) were sampled from a farm in Mount Compass, South Australia in December 2018, during commercial harvest. Matured berries were sampled from four individual plants, with each plant as a replicate. Equal numbers of berries were severed from either the peduncle–pedicel junction (pedicel attached) or from the pedicel–fruit junction (pedicel detached). Samples were transported immediately on ice to the laboratory at the Waite Campus. Blueberries, pedicel attached or detached, were stored, single layer, at 21.8°C with an RH of 63% for 12 h. Berries were weighed before and after storage and weight loss (%) was determined. Blueberry internal $[O_2]$ and tissue vitality were determined.

Internal $[O_2]$ profiles

Fruit (strawberry and blueberry) internal $[O_2]$ was measured using a Clark-type O_2 microelectrode with a tip diameter of 25 μm (OX-25; Unisense A/S, Aarhus, Denmark) with a micromanipulator motorised by SensorTrace Pro (Unisense A/S) as previously described by Xiao *et al.* (2018a, 2018b). The microelectrode was calibrated in a zero O_2 solution (0.1 M NaOH, 0.1 M $C_6H_7NaO_6$) and O_2 saturated (i.e. aerated) Milli-Q water (273 $\mu\text{mol L}^{-1}$ at 22°C, value obtained from Unisense gas table, Ramsing and Gundersen (2021) 'Seawater and gasses – tabulated physical parameters of interest to people working with microsensors in marine systems'). Both strawberries and blueberries were whole and re-equilibrated to ambient temperature before measurement, under laboratory lighting condition. The skin of the fruit was pierced open gently with a stainless-steel syringe needle (19 G) to a depth of approximately 0.2 mm to aid the insertion of the microelectrode into the fruit and to prevent breakage of the microelectrode. For strawberries, $[O_2]$ profiles were obtained in three positions on the fruit: (1) the proximal end longitudinally towards the distal end; (2) the distal end longitudinally towards the proximal end; and (3) the widest point perpendicular towards the central axis (insets of Fig. 1). For blueberries, $[O_2]$ profiles of the fruit were obtained in two positions: (1) the proximal end longitudinally towards the distal end; and (2) the equator inwards to the central axis (inset of Fig. 2). Measurements were taken from 0.2 mm underneath the skin inwards at various increments to different depths depending on the size of the fruit as well as the measuring position on the

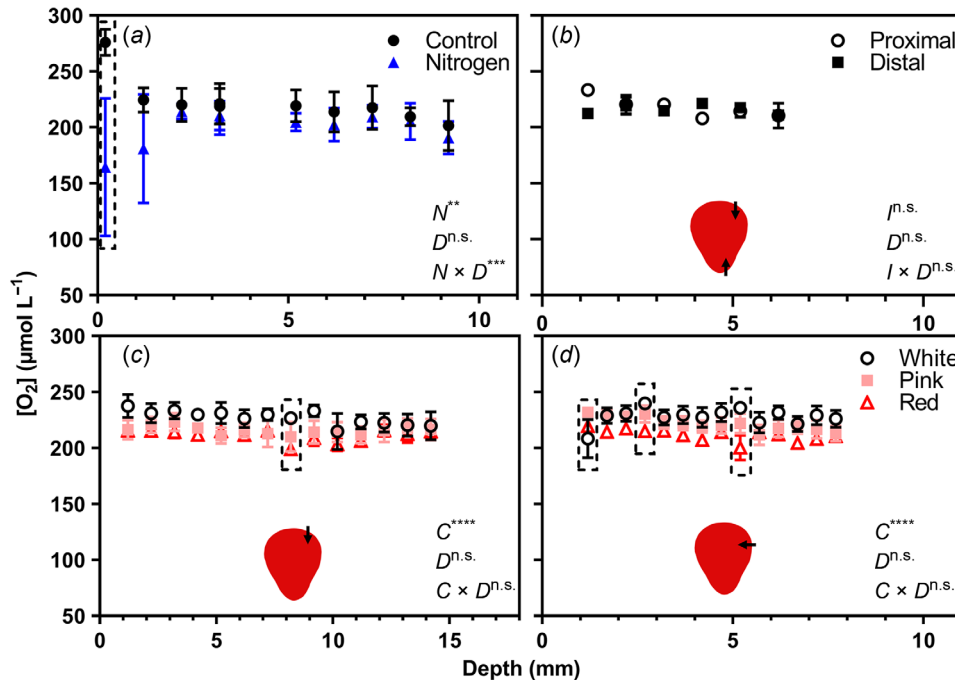


Fig. 1. (a) Comparison of strawberry $[O_2]$ with and without N_2 gas applied at the microelectrode insertion point. The O_2 microelectrode was inserted at the widest point of the strawberry and moved inwards perpendicular towards the central axis. The ANOVA results are given for N_2 gas treatment (N), depth (D) and treatment \times depth ($N \times D$) interaction. Levels of significance are $**P < 0.01$, $***P < 0.001$, $****P < 0.0001$ and n.s., not significant. Sidak's test indicated that N_2 gas lowered the $[O_2]$ to 0.2 mm (dashed rectangle box) ($P < 0.0001$). (b) Strawberry $[O_2]$ profiles from the proximal end longitudinally towards the distal end (\circ) and from the distal end longitudinally towards the proximal end (\blacksquare). The ANOVA results are given for insertion position (I), depth (D) and position \times depth ($I \times D$) interaction. Strawberry $[O_2]$ profiles of three colour ripeness groups, white (\circ), pink (\blacksquare) and red (\triangle), (c) at the proximal end longitudinally towards the distal end and (d) at the widest point perpendicular towards the central axis. The ANOVA results are given for colour ripeness (C), depth (D) and colour \times depth ($C \times D$) interaction. In (c), Sidak's test indicated that $[O_2]$ of the white strawberries was higher than that of the red strawberries at 8.2 mm ($P = 0.03$) (dash-lined rectangle box). In (d), $[O_2]$ of the white strawberries was lower than that of the pink strawberries at 1.2 mm ($P = 0.04$), $[O_2]$ of the white strawberries were higher than those of the red strawberries at 2.7 mm ($P = 0.03$) and 5.2 mm ($P = 0.0008$) (dash-lined rectangle boxes). Fruit temperature at the time of measurement was $20.7 \pm 0.15^\circ\text{C}$, in (c) and (d) ($n = 12$). Error bars are s.e. ($n = 3$ or 4). Insets: arrows indicate the approximate insertion positions of the microelectrode.

fruit. Between each depth, a 20-s waiting time was allowed to ensure stable signals. Further detail of measurement depth for each experiment is specified in the results accordingly. To ensure that insertion of the microelectrode through the fruit tissue did not contaminate the internal $[O_2]$ by the surrounding air, in a separate set of fruit, a gentle stream of nitrogen gas (N_2) was applied to the insertion point during each $[O_2]$ measurement. The readings were compared with those taken at a nearby insertion position where no N_2 was applied. Means and s.e. ($n = 3$ or 4) of each incremented step were calculated and O_2 profiles were compiled using GraphPad Prism 9 (GraphPad Software, San Diego, CA, USA). After the $[O_2]$ measurement, fruit internal temperature was assessed using an infra-red thermometer (Fluke 568;

Fluke Corporation, Everett, WA, USA) with a type-K thermocouple bead probe (Fluke 80PK-1).

Micro-CT

The porosity of selected mesocarp 3D volumes (both proximal and distal regions) in strawberry was measured. Imaging was carried out using a Quantum GX micro-CT (PerkinElmer, Waltham, Massachusetts, USA) ($n = 4$). A total of 803 2D projections were acquired for each strawberry with 0.448° angular steps, at 90 kV/88 μA and scanning time of 14 min. The 2D tomographic images were reconstructed with a voxel resolution of 9 μm (equivalent to $7.3 \times 10^{-7} \text{ mm}^3$ voxel size) from the Quantum GX datasets using the built-in

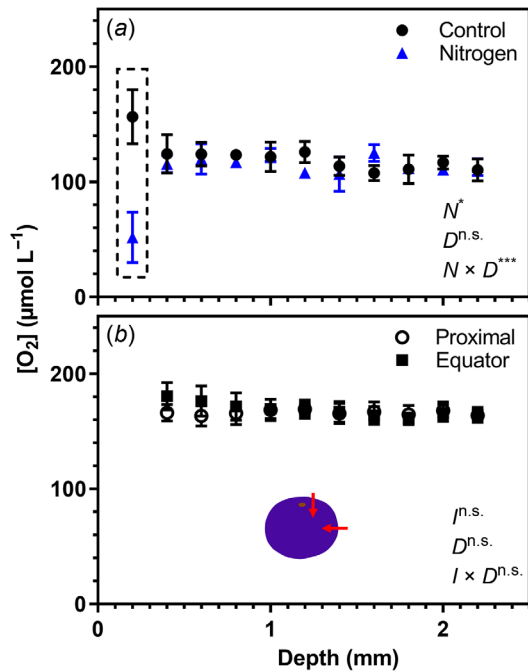


Fig. 2. (a) Comparison of blueberry [O₂] profiles with and without N₂ gas applied at the microelectrode insertion point. The O₂ microelectrode was inserted at the equator and moved inwards perpendicular towards the central axis. The ANOVA results are given for N₂ gas treatment (N), depth (D) and treatment × depth (N × D) interaction. Levels of significance are *P < 0.05, ***P < 0.001 and n.s., not significant. Sidak's test showed N₂ gas lowered the [O₂] at 0.2 mm (dash-lined rectangle box) (P < 0.0001). (b) Blueberry [O₂] profiles at two positions from the proximal end longitudinally towards the distal end (○) and from the equator perpendicular towards the central axis (■). The ANOVA results are given for insertion position (I), depth (D) and position × depth (I × D) interaction. Error bars are s.e. (n = 3 or 4). Inset in (b): arrows indicate the approximate insertion locations of the microelectrode.

software. Using 3D Slicer (ver. 4.11.20200930) (Fedorov *et al.* 2012), the selected volumes of a mesocarp region (i.e. sub-volumes) were specified to exclude the adjacent larger cavities such as the central cavity of the strawberry. The size of the sub-volumes was between approximately 18 and 90 mm³. Differences in X-ray attenuation allowed the application of thresholds to differentiate between void (dark/black area) and organic matter (light/white area). In 3D Slicer, segmentation of intercellular voids was guided by Maximum Entropy automatic thresholding followed by removing extrusions smaller than one voxel, then removing all voids that were less than 500 voxels. The 3D sub-volumes were then assigned a transparent green and the segmented intercellular voids were coloured light yellow. Porosity was defined as the proportion of total intercellular void volume relative to the total volume of the sub-volume, both estimated in 3D Slicer.

Vital staining

A fluorescent diacetate (FDA) staining technique, described in Tilbrook and Tyerman (2008), was used to visually assess cell vitality of the strawberries (red) and blueberries. Esterases within the cytoplasm of vital cells cleave the acetate groups of FDA, turning the molecule fluorescent green. Fluorescent images of stained tissues were examined with a Nikon SMZ 800 (Nikon Co., Tokyo, Japan) dissecting microscope under ultraviolet light with a green fluorescent protein filter in place. Images were obtained using a Nikon DS-5Mc (Tochigi Nikon Precision Co., Ltd, Otawara, Japan) digital camera and NIS-Elements F2.30 software.

Statistics

All statistical analyses were carried out using GraphPad Prism 9. Two-way ANOVA tests, followed by multiple comparison tests where appropriate, were applied to examine the effects of measurement depth and nitrogen gas, insertion position or strawberry colour ripeness on [O₂] measurements. Where [O₂] profiles changed approximately single exponentially as a function of the depth (X, mm) from an initial internal [O₂] (μmol L⁻¹) value beneath the skin barrier, [O₂]₀, to a constant value [O₂]_{const}, the profiles were described by:

$$[\text{O}_2] = ([\text{O}_2]_0 - [\text{O}_2]_{\text{const}})e^{-KX} + [\text{O}_2]_{\text{const}} \quad (1)$$

where K is the rate constant (mm⁻¹). [O₂]₀ was constrained to be less than 273 μmol L⁻¹ (O₂ water saturation at 22°C). Comparison of the fit of one overall curve to the combined data sets and the fit of individual curves to each data set was carried out using the Akaike information criterion (AICc). *t*-Tests were applied to compare weight loss of blueberry after storage and to assess for differences in proximal and distal tissue porosity of strawberry. One-way ANOVA tests were applied to compare TSS and fresh weight between strawberry colour ripeness categories.

Results

A two-way ANOVA test followed by Sidak's test demonstrated that N₂ gas applied, at the location of insertion, lowered [O₂] at 0.2 mm under the skin (P < 0.0001) (Fig. 1a). This indicated that during the time of measurement, N₂ and/or O₂ contamination from the surrounding air did not affect the internal [O₂] profiles of the tissue from 1.2 mm inwards. The [O₂] measurements at both the proximal and distal positions within a same fruit were also similar (Fig. 1b). The three colour ripeness groups of strawberries were similar in weight, 14.1–17.7 g, and in TSS, 6.9–7.7% (Table 1). Strawberries of all colour groups showed consistent [O₂] inwards from near the skin, at each position of the fruit (Fig. 1c, d). In reference to insertion from the proximal end longitudinally

Table 1. Total soluble solids (TSS) and fresh weight of strawberries categorised in three colour ripeness groups.

	TSS (%)	Weight (g)
Green	6.9 ± 0.37	14.7 ± 2.39
Pink	7.5 ± 0.22	14.1 ± 0.41
Red	7.7 ± 0.05	17.7 ± 1.53

One-way ANOVA showed no difference in TSS or weight across ripeness groups. Data are mean ± s.e. ($n = 4$).

towards the distal end, the two-way ANOVA test showed that colour ripeness accounted for 17.85% of total variation ($P < 0.0001$), measurement depth accounted for 5.45% of total variation ($P = 0.73$) and interaction accounted for 4.60% of total variation ($P = 0.99$). The average $[O_2]$ for the white, pink and red strawberries across the same depths were 227 $\mu\text{mol L}^{-1}$, 216 $\mu\text{mol L}^{-1}$ and 211 $\mu\text{mol L}^{-1}$, respectively (Fig. 1c). When assessed from the widest point perpendicular towards the central axis, the two-way ANOVA test showed that colour ripeness accounted for 20.61% of total variation ($P < 0.0001$), measurement depth accounted for 6.05% of total variation ($P = 0.51$) and interaction accounted for 11.26% of total variation ($P = 0.64$). The average $[O_2]$ for the white, pink and red strawberries across the same depths were 228 $\mu\text{mol L}^{-1}$, 222 $\mu\text{mol L}^{-1}$ and 212 $\mu\text{mol L}^{-1}$, respectively (Fig. 1d).

In blueberries, Sidak's test showed that N_2 gas applied at the site of insertion lowered $[O_2]$ at 0.2 mm under the skin ($P < 0.0001$, Fig. 2a), indicating that N_2 and/or O_2 contamination from the surrounding air did not affect the internal $[O_2]$ profiles of the tissue from 0.4 mm inwards. The $[O_2]$ measurements at both positions within a same fruit were also similar (Fig. 2b). It was not feasible to carry out $[O_2]$ measurement on blueberries before softening due to the potential of damaging the oxygen sensor tip. The fitted exponential functions showed that the internal $[O_2]$ in both strawberries and blueberries were relatively consistent across the measured depths and were well above the overall $[O_2]$ in grape berries (Fig. 3, Table 2). Strawberries and blueberries were not internally hypoxic (i.e. minimum $[O_2]$ above the K_m for cytochrome *c* oxidase (0.14 μM) (Millar et al. 1994)), contrary to wine grapes, within which $[O_2]$ can drop to 0 $\mu\text{mol L}^{-1}$ during late ripening (Fig. 3, Table 2). Excised strawberry mesocarp tissues stained with FDA were fluorescent under UV, signifying a high level of cell vitality (Fig. 4).

After 40 h storage, strawberries consistently maintained a non-hypoxic internal status, and a slight drop in $[O_2]$ occurred from near the skin towards the inside of the fruit (no weight loss was observed in strawberries stored at either 4°C or 20°C) (Fig. 5). Noticeably, cold storage (4°C) resulted in higher $[O_2]$ across the measured region under the skin, at both positions on the fruit, relative to those strawberries stored at 20°C (Fig. 5, Table 2, see Supplementary Fig. S1). For cold-stored fruit, from the proximal end longitudinally towards the

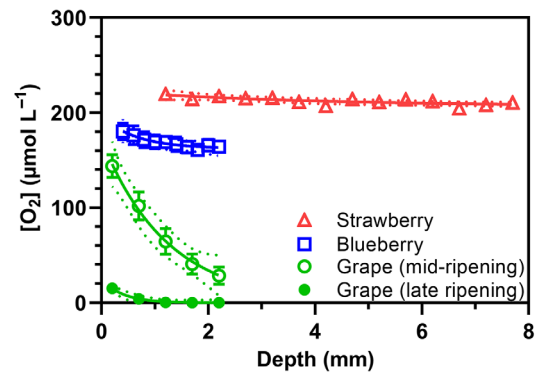


Fig. 3. Internal $[O_2]$ profiles of strawberry (Δ), blueberry (\square) or grape at mid- (\circ) or late ripening (\bullet). Grape $[O_2]$ profiles are from Xiao et al. (2018a). The $[O_2]$ profiles were modelled (with 95% confidence interval) using Eqn 1 (Table 2) and the AICc gives a probability of >99.99% that individual curves fit each dataset. Error bars are s.e. ($n = 3$ or 4).

distal end, the $[O_2]_{\text{const}}$ was 205 $\mu\text{mol L}^{-1}$ (Fig. 5a, Table 2). Across the same depths, at the same position, the $[O_2]_{\text{const}}$ was around 175 $\mu\text{mol L}^{-1}$ for fruit stored at 20°C (Fig. 5a, Table 2). From the widest point perpendicular towards the central axis, the $[O_2]_{\text{const}}$ in the cold-stored fruit was around 209 $\mu\text{mol L}^{-1}$, whereas the $[O_2]_{\text{const}}$ for the 20°C stored strawberries decreased to around 177 $\mu\text{mol L}^{-1}$ (Fig. 5b, Table 2).

After 12 h storage at 21.8°C, the weight loss of blueberries with intact pedicels was less (2.5%) than those that had no pedicels (2.9%) (Fig. 6). A high level of cell vitality was found in blueberries, as indicated by the highly fluorescent FDA-stained tissues (Fig. 6). Pedicel-attached fruit had higher internal $[O_2]$ compared to fruit with no pedicels, as indicated by different exponential functions fitted to the internal $[O_2]$ profiles (Fig. 7, Table 2, Supplementary Fig. S2).

The 2D tomographic images of cross-sections of the strawberry show the location of the central cavity (Fig. 8a) as well as small intercellular voids (i.e. dark/black areas) (Fig. 8a, c). Intercellular voids were visualised and quantified within the mesocarp tissue (i.e. sub-volumes) of the strawberry (Fig. 8b, d). Porosity of the mesocarp of red strawberries declined from 8.61% at the proximal end to 0.41% at the distal region (Fig. 8b, d).

Discussion

The minimum $[O_2]$ of freshly harvested strawberry and blueberry remained above 200 $\mu\text{mol L}^{-1}$ and 160 $\mu\text{mol L}^{-1}$, respectively. This contrasts with the grape berry, which became hypoxic (0–15 $\mu\text{mol L}^{-1}$) during late ripening (Xiao et al. 2018a). Grapes, strawberry and blueberry are non-climacteric fruit with no dramatic changes in respiration during late ripening (Kuhn et al. 2013; Oh et al. 2018; Chen et al. 2020). However, O_2 gradients occur within most fruit

Table 2. Summary of best fit values of Eqn 1 fitted to $[O_2]$ profiles in respective figures.

Figure no.	Dataset	AICc preferred fit (probability)	$[O_2]_0$	$[O_2]_{const}$	K
Fig. 3	Strawberry	Different curve for each data set (>99.99%)	223	207	0.27
	Blueberry		197	162	1.55
	Grape mid		172	0	0.81
	Grape late		26	0	2.59
Fig. 5a	4°C	Different curve for each data set (>99.99%)	239	205	0.40
	20°C		195	175	0.52
Fig. 5b	4°C	Different curve for each data set (>99.99%)	273	209	0.62
	20°C		220	177	0.43
Fig. 7	Attached	Different curve for each data set (99.19%)	141	98	4.01
	Detached		95	79	0.24

$[O_2]_0$, initial internal $[O_2]$ value ($\mu\text{mol L}^{-1}$); $[O_2]_{const}$, constant $[O_2]$ value; K, rate constant (mm^{-1}).

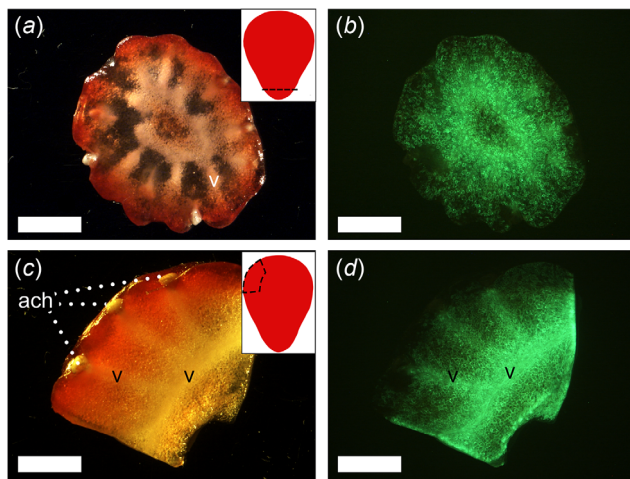


Fig. 4. Images of (a, c) excised strawberry (colour ripeness category: red) tissues and (b, d) their fluorescence with fluorescent diacetate (FDA) staining. Insets show the approximate excision positions by dashed lines. Scale bars are 5 mm. (ach, achenes; v, vascular bundles).

tissues and the steepness of the decreasing gradient depends on internal respiratory demand (Verboven *et al.* 2008) and the tissue's proximity to a locule cavity and/or the tissue porosity (Xiao *et al.* 2018a). The high internal $[O_2]$ of the strawberry was coupled with high mesocarp porosity, likely supporting any respiratory requirement of these cells so that they were found to remain vital here. In seeded Chardonnay grapes, both low berry skin gas permeability and the high respiratory demand of the seeds contributed to the reduced berry internal $[O_2]$ (Xiao *et al.* 2018a). In contrast, strawberries and blueberries have small seeds relative to the size of the fruit, and in the case of the strawberry they are located on the exterior of the fleshy receptacle.

Similar average $[O_2]$ in strawberries between colour ripeness groups suggest any change in respiratory demand within the strawberry may be negligible as the strawberry

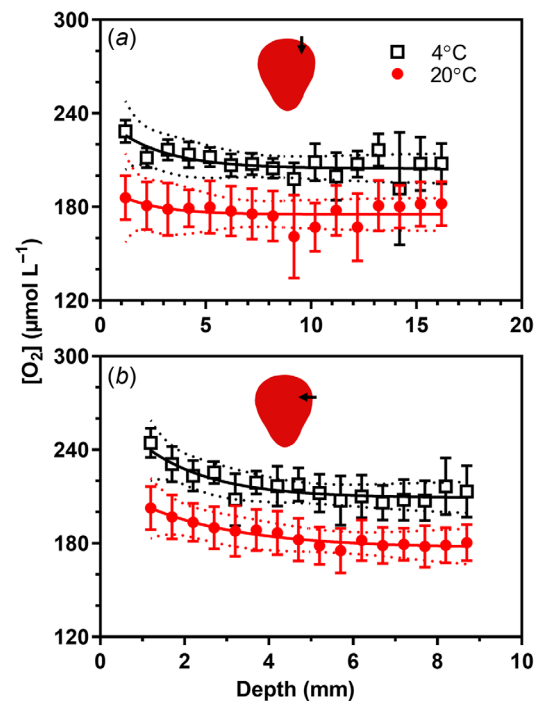


Fig. 5. Strawberry $[O_2]$ profiles after 40 h storage at 20°C (●) (RH = 84%) and 4°C (□) (RH = 83%), (a) from the proximal end longitudinally towards the distal end and (b) from the widest point perpendicular towards the central axis. The $[O_2]$ profiles were modelled (with 95% confidence interval) using Eqn 1 (Table 2) and the AICc gives a probability of >99.99% that individual curves fit each dataset. Fruit temperature at the time of measurement was $22.2 \pm 0.21^\circ\text{C}$ ($n = 8$). Error bars are s.e. ($n = 4$). Insets: arrows indicate the approximate insertion locations of the microelectrode.

matures. However, in contrast to the seeded grape berries, the respiratory increase during ripening resulted in hypoxia, which correlated with mesocarp cell death (Xiao *et al.* 2018a). O_2 diffusivity of fruit internal tissues depends on the amount and connectivity of the intercellular voids (Xiao *et al.* 2021).

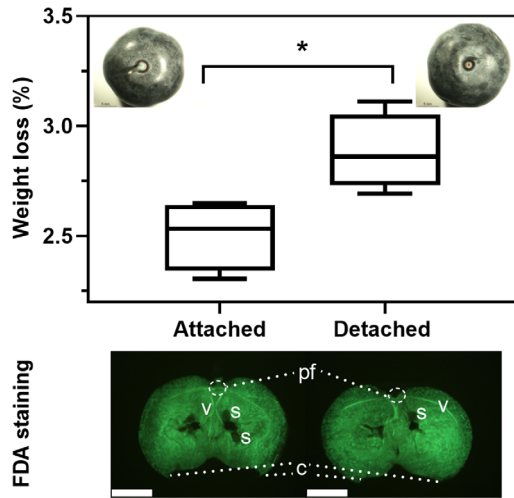


Fig. 6. Weight loss of blueberries stored at 21.8°C (RH = 63%) overnight (12 h) with pedicel attached or detached and examples of fluorescent diacetate (FDA) staining on blueberry longitudinal cross-sections (insets: two pedicel detachment types). Statistical difference is indicated by * (*t*-test, $P = 0.0186$, $n = 4$). Scale bars are 5 mm. (v, vascular bundles; s, seed, c, calyx; pf, pedicel-fruit junction).

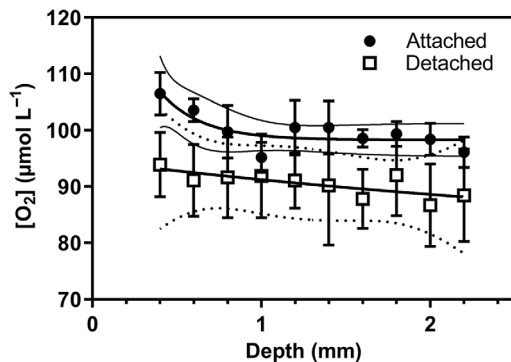


Fig. 7. Blueberry $[O_2]$ profiles after 12 h storage at 21.8°C (RH = 62.9%) with pedicel attached (●) or detached (□) from the proximal end longitudinally towards the distal end. The $[O_2]$ profiles were modelled (with 95% confidence interval) using Eqn 1 (Table 2) and the AICc gives a probability of 99.77% that individual curves fit each dataset. Fruit temperature at the time of measurement was $22.4 \pm 0.10^\circ\text{C}$ ($n = 8$). Error bars are s.e. ($n = 4$).

A considerable volume of intercellular voids was apparent in strawberry receptacle tissues (Fig. 8b, d), potentially facilitating O_2 diffusion within the deeper internal tissue. This contrasts with grape (cv. Shiraz) berries, which were found to show a significant decrease in the amount of intercellular voids in the hypoxic mesocarp during late ripening (Xiao et al. 2018b). Both strawberry and blueberry were reported to have a central cavity and/or locular cavities (Pomper and Breen 1995; Johnson et al. 2011), which may supply O_2 to other internal tissues. This was also exemplified in the tomographic images obtained in this study (Fig. 8a,

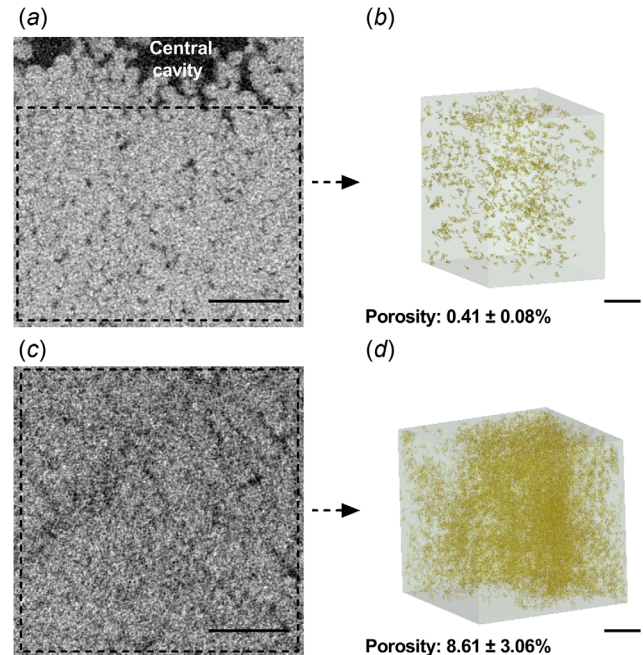


Fig. 8. Tomographic images of the mesocarp of (a, distal and c, proximal) strawberries. Shown are 2D cross-sections obtained at 9 μm voxel resolution. Dark/black areas are intercellular voids and light/white areas are organic matter. The 3D modelling of the intercellular voids in the selected sub-volumes of (b, distal and d, proximal) strawberries [approximate positions of the sub-volumes are demonstrated by dash-lined rectangular boxes (not to scale) in a and c]. Intercellular voids are labelled light yellow within the sub-volumes, marked transparent green. Sub-volumes excluded the larger cavities, such as the central cavity in (a). Scale bars are 1 mm. Porosity is shown as mean \pm s.e., $n = 4$. The *t*-test showed porosity between the distal and proximal sub-volumes were different ($P < 0.05$).

Fig. S3). It was also possible that smaller voids below the segmenting threshold (i.e. less than 500 voxels) may contribute to O_2 availability within the sub-volumes. Both strawberry and blueberry were found to maintain high levels of cell vitality into maturation, and this is likely due to high oxygen diffusivity and availability in the cortex. The high level of cell vitality in the strawberries shown here may facilitate the interdependent development of the receptacle (i.e. the strawberry) and achenes during the late ripening stages (Fait et al. 2008). While organic acids are distributed uniformly through the strawberry, sugar content is usually higher in the apex (distal end) (Enomoto et al. 2018; Ikegaya et al. 2019). Strawberry fruit maintained high internal $[O_2]$ at both distal and proximal ends during development, which suggests oxygen availability is not linked and/or indirectly linked to sugar accumulation and distribution within the cortex. However, lower porosity was found in the distal region and further investigation is warranted to determine if this is related to sugar distribution.

A gentle stream of N_2 was applied to the insertion point of the oxygen sensor to test whether the insertion point could

introduce air into the pierced fruit and therefore affect $[O_2]$ during measurement. The data indicated that the drop in $[O_2]$ caused by N_2 was limited to the measurement point closest to the skin, and at deeper depths there was no impact of the N_2 during the measurement (i.e. within 5 min). The significant drop of $[O_2]$ in the region close to the skin of both fruit when N_2 was applied suggests the insertion point could be leaky to the N_2 stream. However, it is unlikely that leakage of air due to the insertion of the sensor could have resulted in the relatively high overall internal $[O_2]$ in the strawberry and blueberry observed here, since the N_2 gas stream only affected the cell layers from the fruit surface to a depth of 0.2 mm (Figs 1a, 2a).

It is possible that the skin also has high gas permeability. The effectiveness of the formulated air (e.g. increased $[CO_2]$) used to slow the decay of the strawberry, stored in a modified atmosphere (El-Kazzaz *et al.* 1983), could be facilitated by both a porous cortex and a low gas permeation resistant epidermis. To further support this, all tissues (internal or external) can be subjected to respiratory shifts caused by any change in atmospheric composition (Li and Kader 1989; Beaudry *et al.* 1992; Wszelaki and Mitcham 2000). Further study is warranted to determine the efficiency of gas permeability of the epidermis in strawberry and blueberry more accurately. While $[O_2]$ was maintained at similar levels between the depths measured in the present study after short-term storage for both fruit, respiration and homeostasis of the cortex may be disrupted when stored within formulated air due to steepening of the internal $[O_2]$ gradient in prolonged storage. For example, anthocyanin synthesis continues post-harvest in strawberry and in the internal tissue this process was hindered compared to external tissue when subjected to storage in a CO_2 enriched environment for up to 10 days at 5°C (Holcroft and Kader 1999).

When strawberries were stored at 4°C for 40 h, and then allowed to re-equilibrate to ambient temperature, they showed a higher overall internal $[O_2]$ at both the proximal end and the widest point compared to strawberries stored at a constant 20°C. Since the cells remained vital, higher temperature during post-harvest storage likely stimulated respiration (Barrios *et al.* 2014). No weight loss was observed in either storage temperatures and this was likely due to the low vapour pressure deficit (Nunes *et al.* 1998), resulting from the high RH inside the storage containers.

The stem scar contributes to moisture loss during postharvest storage of blueberry (Moggia *et al.* 2017). Indeed, a greater weight loss was observed in blueberries harvested without a pedicel compared to those where the pedicel was attached. A decrease of internal $[O_2]$, as measured at the microelectrode position near the stem scar (i.e. proximal position), was also observed in blueberries with the pedicel detached. The removal of the pedicel, potentially leads to occlusion (e.g. tissue collapse and/or lignification) at the scar site (Moggia *et al.* 2017), may have reduced gas

exchange, since lenticels on the pedicel can act as gas exchange sites between the atmosphere and the fruit (Xiao *et al.* 2018a). Greater water loss could also lead to cells collapsing thereby reducing the volume of intercellular voids and further restricting O_2 availability (Xiao *et al.* 2018b). Green (i.e. chlorophyll containing) pedicels may also contribute to the higher internal $[O_2]$ observed in the pedicel-attached blueberries due to photosynthetic activities (Hetherington *et al.* 1998). These results suggest harvesting blueberries with the pedicel attached could prolong post-harvest quality by retaining fresh weight and intercellular structure.

Conclusion

Fruit internal O_2 status is an important cue for postharvest fruit quality and is associated with fruit internal structure. In the present work, strawberries and blueberries at maturity showed high internal $[O_2]$ most probably due to the extensive intracellular voids and/or proximity to internal cavities. These features could be responsible for the effectiveness of modified storage conditions post-harvest. Lowered storage temperature may decrease respiration of the vital strawberry cortex and the fruit showed higher internal $[O_2]$ when re-equilibrated to ambient temperature. Water loss and O_2 depletion were both reduced by harvesting blueberries with the pedicel attached, an alternative harvesting method with no additional cost. The data presented also demonstrated that the oxygen sensing technique can accurately assess fruit internal $[O_2]$ and could be applied as a rapid-sensing tool that monitors fruit health during storage.

Supplementary material

Supplementary material is available [online](#).

References

- Aday MS, Caner C, Rahvali F (2011) Effect of oxygen and carbon dioxide absorbers on strawberry quality. *Postharvest Biology and Technology* **62**, 179–187. doi:10.1016/j.postharvbio.2011.05.002
- Barrios S, Lema P, Lareo C (2014) Modeling respiration rate of strawberry (cv. San Andreas) for modified atmosphere packaging design. *International Journal of Food Properties* **17**, 2039–2051. doi:10.1080/10942912.2013.784328
- Beaudry RM, Cameron AC, Shirazi A, Dostal-Lange DL (1992) Modified-atmosphere packaging of blueberry fruit: effect of temperature on package O_2 and CO_2 . *Journal of the American Society for Horticultural Science* **117**, 436–441. doi:10.21273/JASHS.117.3.436
- Brown W (1922) On the germination and growth of fungi at various temperatures and in various concentrations of oxygen and of carbon dioxide. *Annals of Botany* **os-36**, 257–283. doi:10.1093/oxfordjournals.aob.a089805
- Chen T, Qin G, Tian S (2020) Regulatory network of fruit ripening: current understanding and future challenges. *New Phytologist* **228**, 1219–1226. doi:10.1111/nph.16822

- Chiabrando V, Giacalone G (2011) Shelf-life extension of highbush blueberry using 1-methylcyclopropane stored under air and controlled atmosphere. *Food Chemistry* **126**, 1812–1816. doi:10.1016/j.foodchem.2010.12.032
- El-Kazzaz MK, Sommer NF, Fortlage RJ (1983) Effect of different atmospheres on postharvest decay and quality of fresh strawberries. *Phytopathology* **73**, 282–285. doi:10.1094/Phyto-73-282
- Enomoto H, Sato K, Miyamoto K, Ohtsuka A, Yamane H (2018) Distribution analysis of anthocyanins, sugars, and organic acids in strawberry fruits using matrix-assisted laser desorption/ionization-imaging mass spectrometry. *Journal of Agricultural and Food Chemistry* **66**, 4958–4965. doi:10.1021/acs.jafc.8b00853
- Fait A, Hanhineva K, Beleggia R, Dai N, Rogachev I, Nikiforova VJ, Fernie AR, Aharoni A (2008) Reconfiguration of the achene and receptacle metabolic networks during strawberry fruit development. *Plant Physiology* **148**, 730–750. doi:10.1104/pp.108.120691
- Fedorov A, Beichel R, Kalpathy-Cramer J, Finet J, Fillion-Robin J-C, Pujol S, Bauer C, Jennings D, Fennessy F, Sonka M, Buatti J, Aylward S, Miller JV, Pieper S, Kikinis R (2012) 3D Slicer as an image computing platform for the Quantitative Imaging Network. *Magnetic Resonance Imaging* **30**, 1323–1341. doi:10.1016/j.mri.2012.05.001
- Hetherington SE, Smillie RM, Davies WJ (1998) Photosynthetic activities of vegetative and fruiting tissues of tomato. *Journal of Experimental Botany* **49**, 1173–1181. doi:10.1093/jxb/49.324.1173
- Ho QT, Verboven P, Mebatsion HK, Verlinden BE, Vandewalle S, Nicolai BM (2009) Microscale mechanisms of gas exchange in fruit tissue. *New Phytologist* **182**, 163–174. doi:10.1111/j.1469-8137.2008.02732.x
- Holcroft DM, Kader AA (1999) Carbon dioxide-induced changes in color and anthocyanin synthesis of stored strawberry fruit. *HortScience* **34**, 1244–1248. doi:10.21273/HORTSCI.34.7.1244
- Hollender CA, Geretz AC, Slovin JP, Liu Z (2012) Flower and early fruit development in a diploid strawberry, *Fragaria vesca*. *Planta* **235**, 1123–1139. doi:10.1007/s00425-011-1562-1
- Ikegaya A, Toyozumi T, Ohba S, Nakajima T, Kawata T, Ito S, Arai E (2019) Effects of distribution of sugars and organic acids on the taste of strawberries. *Food Science & Nutrition* **7**, 2419–2426. doi:10.1002/fsn3.1109
- Johnson LK, Malladi A, NeSmith DS (2011) Differences in cell number facilitate fruit size variation in rabbiteye blueberry genotypes. *Journal of the American Society for Horticultural Science* **136**, 10–15. doi:10.21273/JASHS.136.1.10
- Kader AA, Ben-Yehoshua S (2000) Effects of superatmospheric oxygen levels on postharvest physiology and quality of fresh fruits and vegetables. *Postharvest Biology and Technology* **20**, 1–13. doi:10.1016/S0925-5214(00)00122-8
- Ke D, Goldstein L, O'Mahony M, Kader AA (1991) Effects of short-term exposure to low O₂ and high CO₂ atmospheres on quality attributes of strawberries. *Journal of Food Science* **56**, 50–54. doi:10.1111/j.1365-2621.1991.tb07973.x
- Kuhn N, Guan L, Dai ZW, Wu B-H, Lauvergeat V, Gomès E, Li S-H, Godoy F, Arce-Johnson P, Delrot S (2013) Berry ripening: recently heard through the grapevine. *Journal of Experimental Botany* **65**, 4543–4559. doi:10.1093/jxb/ert395
- Larsen M, Watkins CB (1995) Firmness and concentrations of acetaldehyde, ethyl acetate and ethanol in strawberries stored in controlled and modified atmospheres. *Postharvest Biology and Technology* **5**, 39–50. doi:10.1016/0925-5214(94)00012-H
- Li C, Kader AA (1989) Residual effects of controlled atmospheres on postharvest physiology and quality of strawberries. *Journal of the American Society for Horticultural Science* **114**, 629–634. doi:10.21273/JASHS.114.4.629
- Millar AH, Bergersen FJ, Day DA (1994) Oxygen affinity of terminal oxidases in soybean mitochondria. *Plant Physiology and Biochemistry* **32**, 847–852.
- Moggia C, Beaudry RM, Retamales JB, Lobos GA (2017) Variation in the impact of stem scar and cuticle on water loss in highbush blueberry fruit argue for the use of water permeance as a selection criterion in breeding. *Postharvest Biology and Technology* **132**, 88–96. doi:10.1016/j.postharvbio.2017.05.019
- Nunes MCN, Brecht JK, Morais AMMB, Sargent SA (1998) Controlling temperature and water loss to maintain ascorbic acid levels in strawberries during postharvest handling. *Journal of Food Science* **63**, 1033–1036. doi:10.1111/j.1365-2621.1998.tb15848.x
- Oh HD, Yu DJ, Chung SW, Chea S, Lee HJ (2018) Abscisic acid stimulates anthocyanin accumulation in 'Jersey' highbush blueberry fruits during ripening. *Food Chemistry* **244**, 403–407. doi:10.1016/j.foodchem.2017.10.051
- Pomper KW, Breen PJ (1995) Levels of apoplastic solutes in developing strawberry fruit. *Journal of Experimental Botany* **46**, 743–752. doi:10.1093/jxb/46.7.743
- Pott DM, Vallarino JG, Osorio S (2020) Metabolite changes during postharvest storage: effects on fruit quality traits. *Metabolites* **10**, 187. doi:10.3390/metabo10050187
- Ramsing NB, Gundersen JK (2021) Seawater and gasses: tabulated physical parameters of interest to people working with microsensors in marine systems: unisense data tables. Available from Unisense A/S, Denmark at <https://unisense.com/wp-content/uploads/2021/10/Seawater-Gases-Table.pdf> [accessed 2021]
- Rodriguez J, Zoffoli JP (2016) Effect of sulfur dioxide and modified atmosphere packaging on blueberry postharvest quality. *Postharvest Biology and Technology* **117**, 230–238. doi:10.1016/j.postharvbio.2016.03.008
- Schotsmans W, Molan A, MacKay B (2007) Controlled atmosphere storage of rabbiteye blueberries enhances postharvest quality aspects. *Postharvest Biology and Technology* **44**, 277–285. doi:10.1016/j.postharvbio.2006.12.009
- Tilbrook J, Tyerman SD (2008) Cell death in grape berries: varietal differences linked to xylem pressure and berry weight loss. *Functional Plant Biology* **35**, 173–184. doi:10.1071/FP07278
- Vashisth T, Malladi A (2013) Fruit detachment in rabbiteye blueberry: abscission and physical separation. *Journal of the American Society for Horticultural Science* **138**, 95–101. doi:10.21273/JASHS.138.2.95
- Verboven P, Kerckhofs G, Mebatsion HK, Ho QT, Temst K, Wevers M, Cloetens P, Nicolai BM (2008) Three-dimensional gas exchange pathways in pome fruit characterized by synchrotron X-ray computed tomography. *Plant Physiology* **147**, 518–527. doi:10.1104/pp.108.118935
- Wszelaki AL, Mitcham EJ (2000) Effects of superatmospheric oxygen on strawberry fruit quality and decay. *Postharvest Biology and Technology* **20**, 125–133. doi:10.1016/S0925-5214(00)00135-6
- Xiao Z, Rogiers SY, Sadras VO, Tyerman SD (2018a) Hypoxia in grape berries: the role of seed respiration and lenticels on the berry pedicel and the possible link to cell death. *Journal of Experimental Botany* **69**, 2071–2083. doi:10.1093/jxb/ery039
- Xiao Z, Liao S, Rogiers SY, Sadras VO, Tyerman SD (2018b) Effect of water stress and elevated temperature on hypoxia and cell death in the mesocarp of Shiraz berries. *Australian Journal of Grape and Wine Research* **24**, 487–497. doi:10.1111/ajgw.12363
- Xiao H, Piovesan A, Pols S, Verboven P, Nicolai B (2021) Microstructural changes enhance oxygen transport in tomato (*Solanum lycopersicum*) fruit during maturation and ripening. *New Phytologist* **232**, 2043–2056. doi:10.1111/nph.17712

Data availability. The data that support this study are available in the article and accompanying online supplementary material.

Conflicts of interest. The authors declare no conflicts of interest.

Declaration of funding. This work was supported by the Gulbali Institute, Charles Sturt University and Australian Research Council Training Centre for Innovative Wine Production, funded by the Australian Government (IC170100008) with additional support from Wine Australia and industry partners.

Acknowledgements. The authors thank Ms Wendy Sullivan, Dr Scott Willis and Ms. Helen Pan for expert technical assistance and acknowledge the facilities and assistance of the University of Adelaide and the National Imaging Facility at the Biomedical Magnetic Resonance Facility, Western Sydney University. The authors thank The Beerenberg Family Farm (SA), Berrylicious Strawberries (NSW) and The Blueberry Patch (SA) for sampling at their farms.

Author affiliations

^AAustralian Research Council Training Centre for Innovative Wine Production, Glen Osmond, SA 5064, Australia.

^BGulbali Institute, Charles Sturt University, Wagga Wagga, NSW 2678, Australia.

^CNanoscale Organisation and Dynamics Group, Western Sydney University, Penrith, NSW 2751, Australia.

^DDepartment of Wine Science and Waite Research Institute, The University of Adelaide, Glen Osmond, SA 5064, Australia.

^ENew South Wales Department of Primary Industries, Wollongbar, NSW 2477, Australia.